INTERNATIONAL JOURNAL FOR NUMERICAL METHODS IN FLUIDS, VOL. 17, 99–113 (1993)

THE BEHAVIOUR OF SEVERAL STRESS–VELOCITY–PRESSURE MIXED FINITE ELEMENTS FOR NEWTONIAN FLOWS

GUSTAVO C. BUSCAGLIA
Div. Mecánica Computacional, DIA, Centro Atómico Bariloche, CNEA, 8400 – S.C. de Bariloche – Argentina

SUMMARY

The Q_2/P_1, P_2^+/P_1, P_2/P_0 and Q_1/P_0 velocity–pressure mixed elements are extended to the stress–velociy–pressure formulation, using the same interpolants for stress and velocity, and tested in the 4-to-1 contraction problem for Stokes flow. The comparison shows significant differences among them, which are not present when the velocity–pressure formulation is used.

To provide a better understanding of the phenomenon, several variants of the previous elements are introduced, obtained by either changing the pressure space or by enriching the stress space with bubble functions. The formulation exhibits a strong sensitivity to the first alternative, while the second produces only a minor effect. These observations are confirmed by a convergence test effected on a regular problem with the explicit analytical solution. Also, as a result of the whole comparison, the $P_2^+/P_2^+/P_1$ element looks promising for three-field calculations.

1. INTRODUCTION

In this paper we deal with the stress–velocity–pressure formulation of the Stokes problem, which has received increasing attention during the last years.[1–8] The motivation for this has come from the area of viscoelastic flow simulation, where the extra-stresses cannot be eliminated at the exact problem level and a three-field formulation is, thus, unavoidable. In the early and fundamental papers of Crochet and Marchal,[6,7] it was recognized that a mixed finite element that works properly in the Newtonian limit is a necessary (although unfortunately not sufficient) condition for successful simulation of highly elastic liquids. In particular, of primary interest are those elements with continuous (C^0) approximation for the stress, because this allows the use of Newton's iterations to deal with the non-linearities that occur in the constitutive equation.

In this work we study the numerical performance of several three-field mixed finite elements of this kind, obtained essentially by using the same interpolants for velocity and extra-stress components. This allows a fruitful comparison of various possibilities, identifying those combinations that behave poorly. To understand better these results, we consider elements that differ only in either the pressure space or the extra-stress one, so as to gain some insight into the interplay among the discrete spaces.

The plan of this paper is as follows: In Section 2 the exact problem and its variational formulation is presented. The approximation method, together with the basic mixed elements to be studied are described in Section 3. Section 4 contains the numerical results as obtained with the

0271–2091/93/140099–15$12.50

Received March 1992
Revised November 1992

elements of Section 3. We then turn to consider some variants of the original elements, which are presented and tested in Section 5. A numerical convergence analysis is carried out in Section 6. Some overall conclusions are drawn in Section 7.

2. THREE-FIELD FORMULATION OF THE STOKES PROBLEM

In this work, we will deal with a three-field formulation of the Stokes problem that appears as the zero-elasticity limit of viscoelastic models that include an additional viscosity (the same formulation has been studied in Reference 1). The classical formulation can be obtained making this additional or solvent viscosity μ_2 take zero value. The governing equations are, in differential form:

$$-\mu_2 \nabla^2 v - \operatorname{div} \tau + \nabla p = f, \tag{1}$$

$$\operatorname{div} v = 0, \tag{2}$$

$$\tau - 2\mu_1 D v = 0, \tag{3}$$

where v stands for the velocity field, τ for the extra-stress tensor, p for the pressure, Dv for the strain rate tensor and f for the body forces. It is clear that, replacing (3) in (1), the classical velocity–pressure formulation of the Stokes problem, with viscosity equal to $\mu_1 + \mu_2$ is recovered. For that reason, the usual boundary conditions of specified velocities (Dirichlet type) or boundary forces (Neumann type) are required.

Let Ω be the (bounded) domain of interest, $\Sigma = [L^2(\Omega)]_s^4$ be the space of symmetric 2×2 tensors, $V = [H_0^1(\Omega)]^2$ be the space two-dimensional vector fields with square-integrable derivatives that vanish at the boundaries, and $Q = L_0^2(\Omega)$ be the space of square integrable functions with zero integral. For simplicity, we are restricting to homogeneous Dirichlet boundary conditions. An appropriate variational form of (1)–(3) is, thus,

Find $(v, p, \tau) \in V \times Q \times \Sigma$, such that

$$\int_\Omega (2\mu_2 D v + \tau) : D w \, d\Omega - \int_\Omega p \operatorname{div} w \, d\Omega = \int_\Omega f w \, d\Omega, \quad \forall w \in V, \tag{4}$$

$$\int_\Omega q \operatorname{div} v \, d\Omega = 0, \quad \forall q \in Q, \tag{5}$$

$$\int_\Omega (\tau - 2\mu_1 D v) : \chi \, d\Omega = 0, \quad \forall \chi \in \Sigma. \tag{6}$$

3. FINITE ELEMENT APPROXIMATION

It is quite natural to discretize (4)–(6) introducing the finite element spaces

$$V_h \subset V, \qquad Q_h \subset Q, \qquad \Sigma_h \subset \Sigma$$

and restricting the variational problem to these subspaces. If $\mu_2 > 0$, it can be readily shown that existence and uniqueness of the discrete problem is obtained, whenever the well-known Babuska–Brezzi or inf–sup condition over V_h and Q_h holds. Moreover, convergence to the exact solution with optimal order as h tends to zero can be proved.[1] In the limit of zero μ_2, another

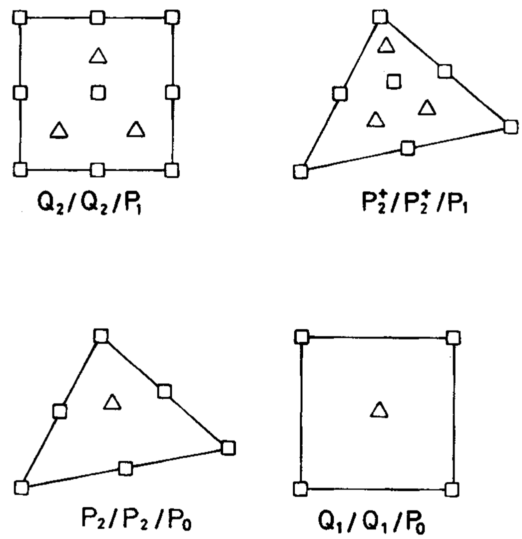

Figure 1. The four basic mixed elements to be compared (□ stress–velocity node, Δ pressure node)

inf–sup condition is required, namely,

$$\inf_{w\in X_h}\sup_{\sigma\in\Sigma_h}\frac{\int_\Omega \sigma\colon Dw\,\mathrm{d}\Omega}{\|w\|\;\|\sigma\|}\geq\beta>0, \tag{7}$$

where the norms of w and σ are those of V and Σ, respectively, and

$$X_h=\left\{w\in V_h\Big/\int_\Omega q\operatorname{div} w\,\mathrm{d}\Omega=0\quad\text{for all } q\in Q_h\right\}. \tag{8}$$

Let us now introduce four basic mixed elements which will be considered in the sequel (see also Figure 1). Some possible variants will be discussed in later sections. *All of them have continuous interpolants for stress and velocity, while the pressure is approximated by discontinuous functions.* The label assigned to each element is formed by the usual notation for interpolants, in the following order: extra-stress–velocity–pressure.

1. *Biquadratic/biquadratic/linear* ($Q_2/Q_2/P_1$): In this case, the Q_2/P_1 element, known to perform very well for the velocity–pressure formulaton, is used. Complete biquadratic interpolants approximate the velocity inside each element, while piecewise linear discontinuous interpolants are used for the pressure. For each component of τ, also biquadratic basis functions are used (this element has also been considered in Reference 8).
2. *Enriched quadratic/enriched quadratic/linear* ($P_2^+/P_2^+/P_1$): This is another element that works very well for the velocity–pressure formulation. Velocities are approximated by qadratic functions inside each element, with the addition of a bubble function for stability. Pressure is approximated by discontinuous piecewise linear functions. Again, the τ components have the same interpolants as the velocity components.
3. *Quadratic/quadratic/constant* ($P_2/P_2/P_0$): This element is very similar to the previous one. However, to satisfy the Babuska–Brezzi condition without adding bubbles, the pressure space must be reduced just to piecewise constant functions, thus loosing h-convergence

order. In fact, combining P_2 velocities with linear discontinuous pressure leads to the well-known checkerboard effect typical of spurious pressure modes.

4. *Bilinear/bilinear/constant* ($Q_1/Q_1/P_0$): In this case, the well-known Q_1/P_0 element is used for velocity and pressure. Although this combination does not satisfy the Babuska–Brezzi condition, it is known to yield good results. Each component of τ is also interpolated with Q_1 approximation.

4. NUMERICAL EXPERIMENTS WITH THE FOUR BASIC ELEMENTS

We will restrict ourselves to a quite standard model problem in this section, the 4-to-1 plane contraction, which will thus be only briefly described. The computational domain and the meshes chosen are not intended to provide precise results, but just to allow for performance comparison. *To avoid unnecessary parameters we will keep $\mu_1 + \mu_2$ equal to one in all the experiments.*

With the contraction line situated at $x_2 = 0$, the domain extends from $x_2 = -4$ to $x_2 = +4$. At the inlet, a fully developed velocity profile with mean velocity equal to 0·25 is imposed, so that the mean velocity at the outlet is 1. At the outlet, the horizontal velocity is specified as zero.

We will use the meshes of Figure 2 for biquadratic quadrilaterals. For bilinear quadrilaterals each element is subdivided into four equal ones. In the case of quadratic triangles, each rectangle of Figure 2 is divided into two triangles by joining the lower-left and upper-right corners. In this way, whatever the element is considered, we will compare results obtained with the same number of stress–velocity nodes (exception made of bubble-type unknowns).

As all of the elements considered are known to perform well in the velocity–pressure formulation (which in our formulation corresponds to $\mu_1 = 0$ and $\mu_2 = 1$), our interest is focused in the region of small μ_2. As μ_2 goes to zero, the theoretical results of Reference 1 cease to apply, and we are left with the *open* problem of whether the elements considered are stable or not in this limit.

To study this, we put $\mu_1 = 0{\cdot}999$, $\mu_2 = 0{\cdot}001$ and obtain the results of Figures 3–5, corresponding to the $Q_2/Q_2/P_1$, $P_2^+/P_2^+/P_1$ and $Q_1/Q_1/P_0$ elements, respectively. In these figures, we have plotted the horizontal velocity (v_1) and vertical normal extra-stress (τ_{22}) contours as computed

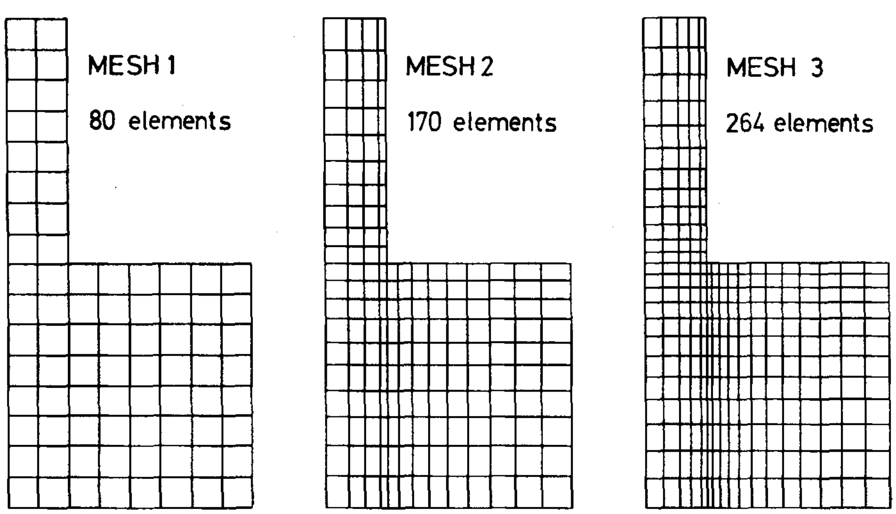

Figure 2. Meshes for the 4-to-1 contraction problem

on the three meshes of Figure 2. The comparison shows that the $P_2^+/P_2^+/P_1$ is much more robust than the other two, which present mesh-sized oscillations which are (at least) very hard to remove by mesh refinement.

Observation: A reference computation made on a very fine mesh using a standard Navier–Stokes solver yielded minimum and maximum values for v_1 of $-0{\cdot}3324$ and $0{\cdot}2101 \times 10^{-2}$, respectively (to be compared with the values reported in the figures).

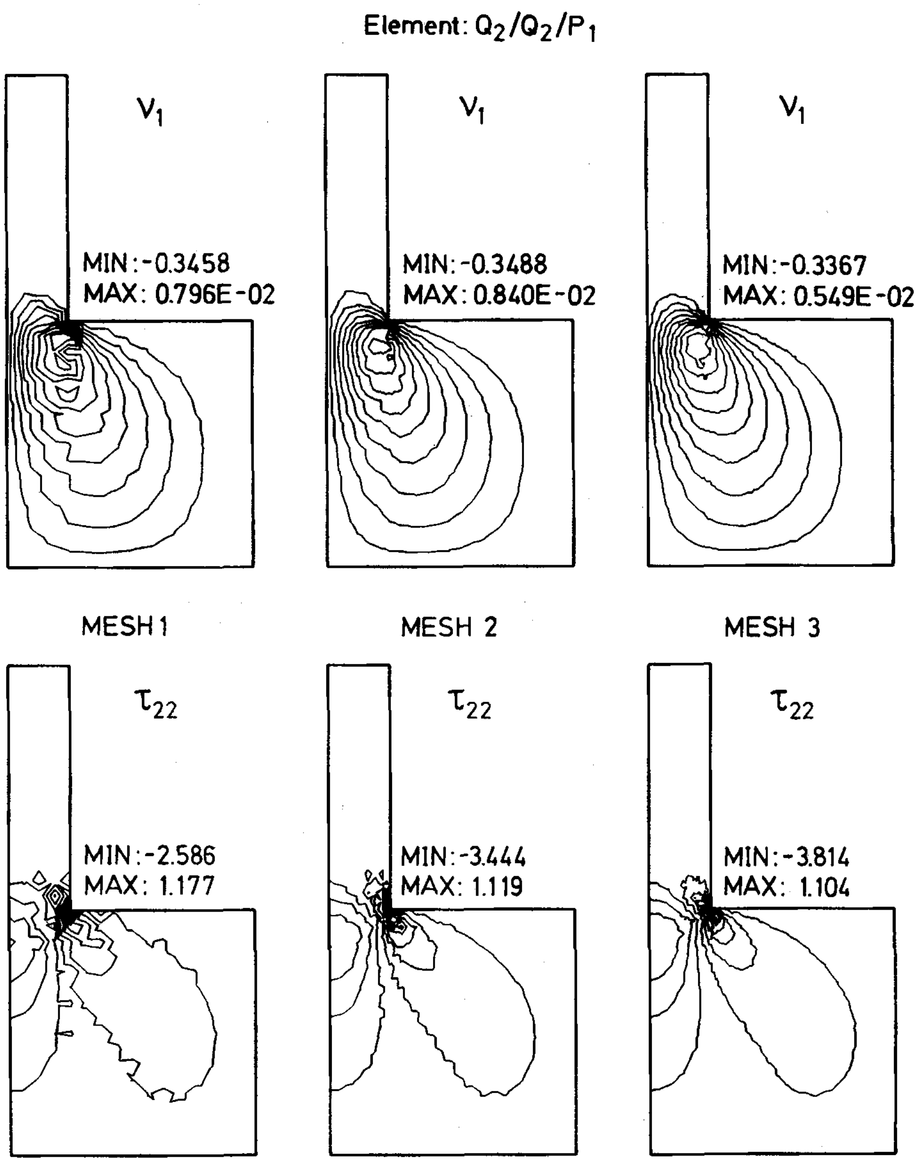

Figure 3. v_1 and τ_{22} contours as obtained with the $Q_2/Q_2/P_1$ element on the three meshes of Figure 2. We have taken $\mu_1 = 0{\cdot}999$ and $\mu_2 = 0{\cdot}001$

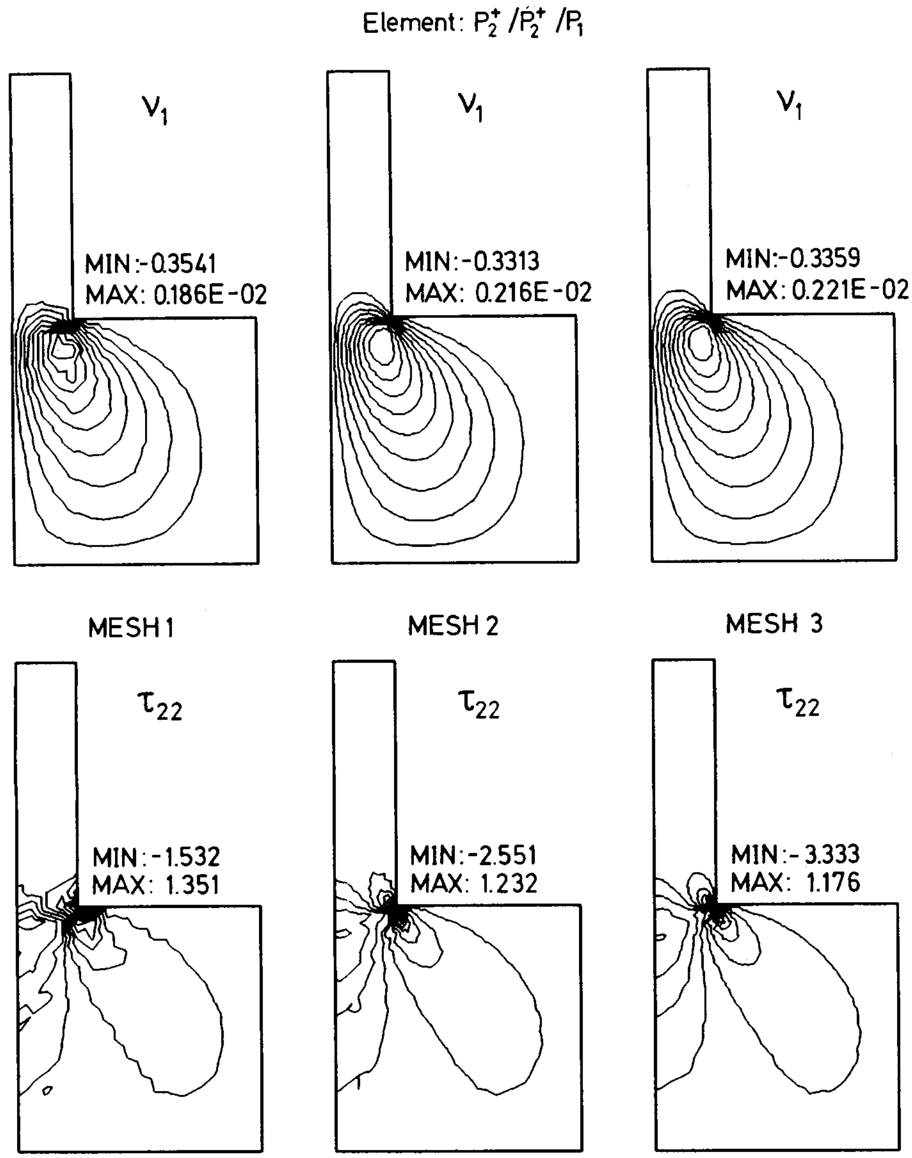

Figure 4. Performance of the $P_2^+/P_2^+/P_1$ element (as in Figure 3)

However, even if the performance of the basic quadrilaterals is not optimal, it is infinitely better than that of the $P_2/P_2/P_0$ element, which is clearly unstable (Figure 7(a) shows the corresponding v_1 contours as obtained with MESH 3). We have to stress at this point that none of the above pathologies persists when μ_2 increases and, thus, they clearly come from a poor (at best) satisfaction of condition (7).

The unstructured nature of triangular meshes also allowed us to continue the refinement in the vicinity of the re-entrant corner. Although this results are not included for brevity reasons, they confirm the robustness of the $P_2^+/P_2^+/P_1$ element, with no sensitivity to abrupt mesh-size changes.

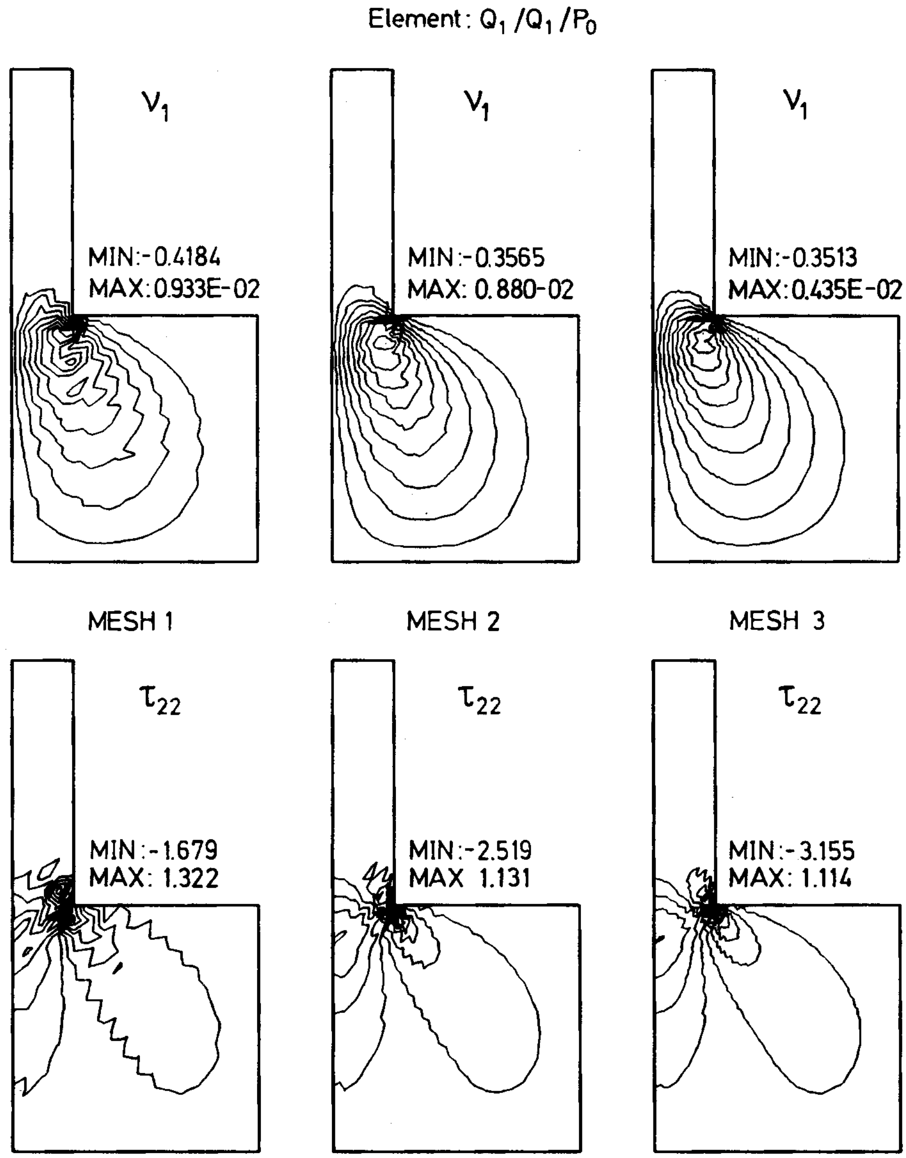

Figure 5. Performance of the $Q_1/Q_1/P_0$ element (as in Figure 3)

5. SOME VARIANTS OF THE FOUR BASIC ELEMENTS

A full explanation of the results of the previous section is far beyond our goals (and knowledge). Nevertheless, as current research in the numerical analysis of the Stokes problem (mainly motivated by viscoelastic flow simulation) concerns the stability and convergence properties of the three discrete spaces coupled by the variational problem ((4)–(6)), it is interesting to investigate some variants of the four basic elements obtained by modifying this spaces at will.

We divide this section in two main parts. In one of them we study the effects of changing the discrete pressure space, thus strengthening or weakening the incompressibility constraint. In the

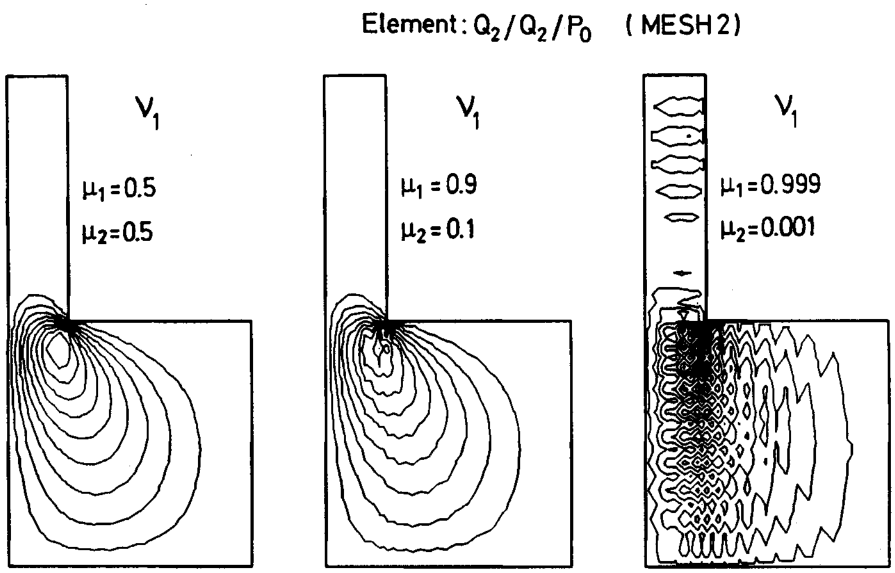

Figure 6. Unstable behaviour of the $Q_2/Q_2/P_0$ element when μ_2 approaches zero

other, we consider the effects of adding bubbles to the stress space but not to the velocity one. In turn, this can be regarded as allowing the constitutive equation (6) to be better fulfilled than the dynamic equilibrium equation (4) (correspondingly, equations (3) and (1) for the differential formulation).

5.1. The effect of the incompressibility constraint

We will consider here two mixed elements: the $Q_2/Q_2/P_0$ square and the $P_2^+/P_2^+/P_0$ triangle. These are to be compared with their linear-pressure counterparts already presented. When μ_1 is small, both of them yield acceptable results with the meshes of Figure 2. Increasing μ_1 strongly deteriorates both the stress and the velocity fields, while the pressure remains smooth.

To illustrate this loss of accuracy, we show in Figure 6 the horizontal velocity contours, as obtained with the $Q_2/Q_2/P_0$ element with $\mu_1=0{\cdot}5$ (Figure 6(a)), 0·9 (Figure 6(b)) and 0·999 (Figure 6(c)) on MESH 2. The behaviour of the $P_2^+/P_2^+/P_0$ triangle, with $\mu_1=0{\cdot}999$ on MESH 3 can be seen in Figure 7(c).

Observing the resemblance of the results obtained with the $P_2/P_2/P_0$ and the $P_2^+/P_2^+/P_0$ triangles, the performance of the former becomes less surprising. However, the reported phenomena cannot be considered an effect of P_0 pressure approximation alone, as the $Q_1/Q_1/P_0$ seems to be free of this instability. Heuristically, one could suggest that this phenomenon comes from the discrete incompressibility constraint being *too weak* for the corresponding velocity–stress approximation (this will be more rigorously discussed in the next section).

To verify this assertion, we conducted one further comparison. As the pressure space of the $Q_1/Q_1/P_0$ cannot be further reduced, the obvious alternative is to enrich the stress and velocity spaces. To do this, we added a bubble function to the Q_1 interpolants, obtained by multiplying two shape functions corresponding to opposite nodes of the master element so that the result vanishes at element boundaries. This extended-Q_1-approximation will be labelled Q_1^+.

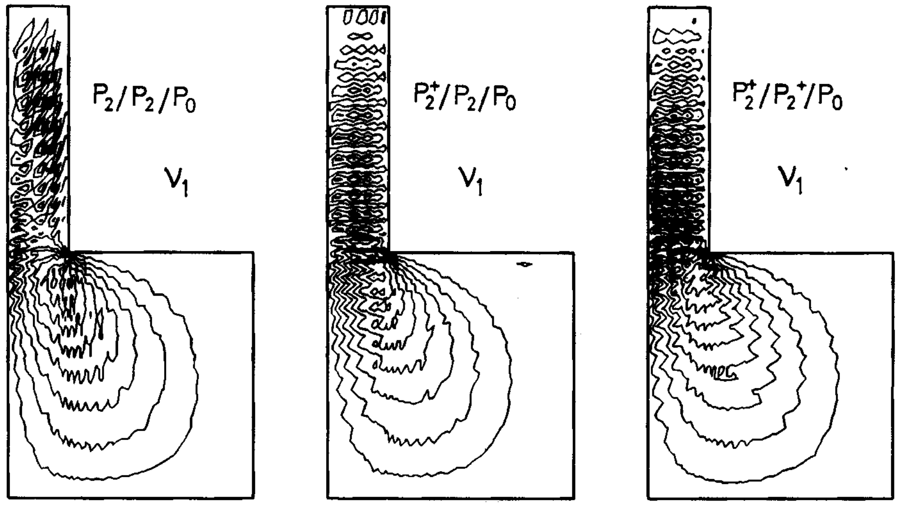

Figure 7. Unstable behaviour of quadratic/quadratic/constant triangles. The instability cannot be cured by adding bubble functions. The results correspond to $\mu_1=0{\cdot}999$, $\mu_2=0{\cdot}001$ and MESH 3

The results are consistent with our conjecture. To show this, we plot in Figure 8 the v_1 and τ_{22} contours when $\mu_1=0{\cdot}999$ for the three meshes. Clearly, an oscillatory mesh-sized mode appears which is nevertheless reduced by mesh refinement. The convergence analysis of Section 6 will eventually show that this element does not converge.

5.2. *The effect of enriching the stress space with bubble functions*

Contrary to our expectations, we have not observed such a tight coupling between stresses and velocities as that observed between pressure and the other fields. When μ_1 is small, this can be attributed to the stabilizing effect of the μ_2 viscosity, but the same is observed with μ_1 near unity.

Consider the $P_2/P_2/P_0$ element. Its behaviour was discussed in Section 4. Changing the stress space to P_2^+ (i.e. switching to the $P_2^+/P_2/P_0$ element) yields different but not better results. Indeed, taking $\mu_1=0{\cdot}98$ in the 4-to-1 contraction, the three elements $P_2/P_2/P_0$, $P_2^+/P_2/P_0$ and $P_2^+/P_2^+/P_0$ behave approximately in the same way, the latter performing slightly worse. Some differences arise in the velocity field when $\mu_1=0{\cdot}999$ (see Figure 7), suggesting that they are not equivalent in the limit, but we did not investigate this further.

Turning now to the $Q_1/Q_1/P_0$ element, we have already shown in Figure 8 the effect of enriching both the stress and the velocity spaces. If only the stresses are enriched, the results are in between, perhaps closer to the $Q_1^+/Q_1^+/P_0$ case, but with no significant changes (see Figure 9).

Finally, let us consider the $P_2^+/P_2^+/P_1$ element, as compared with the $P_2/P_2^+/P_1$ variant (recently used by Hulsen[9]). Even when μ_2 is small, both elements behave in a very similar way, again showing the weak sensitivity of the three-fields formulation to the addition of bubble functions to the discrete-stress space.

6. NUMERICAL CONVERGENCE ANALYSIS

To study the convergence of the mixed elements presented above, we have selected a rather academic problem with a very attractive property: It has an explicit polynomic solution which is not contained in any of the finite element spaces we consider.

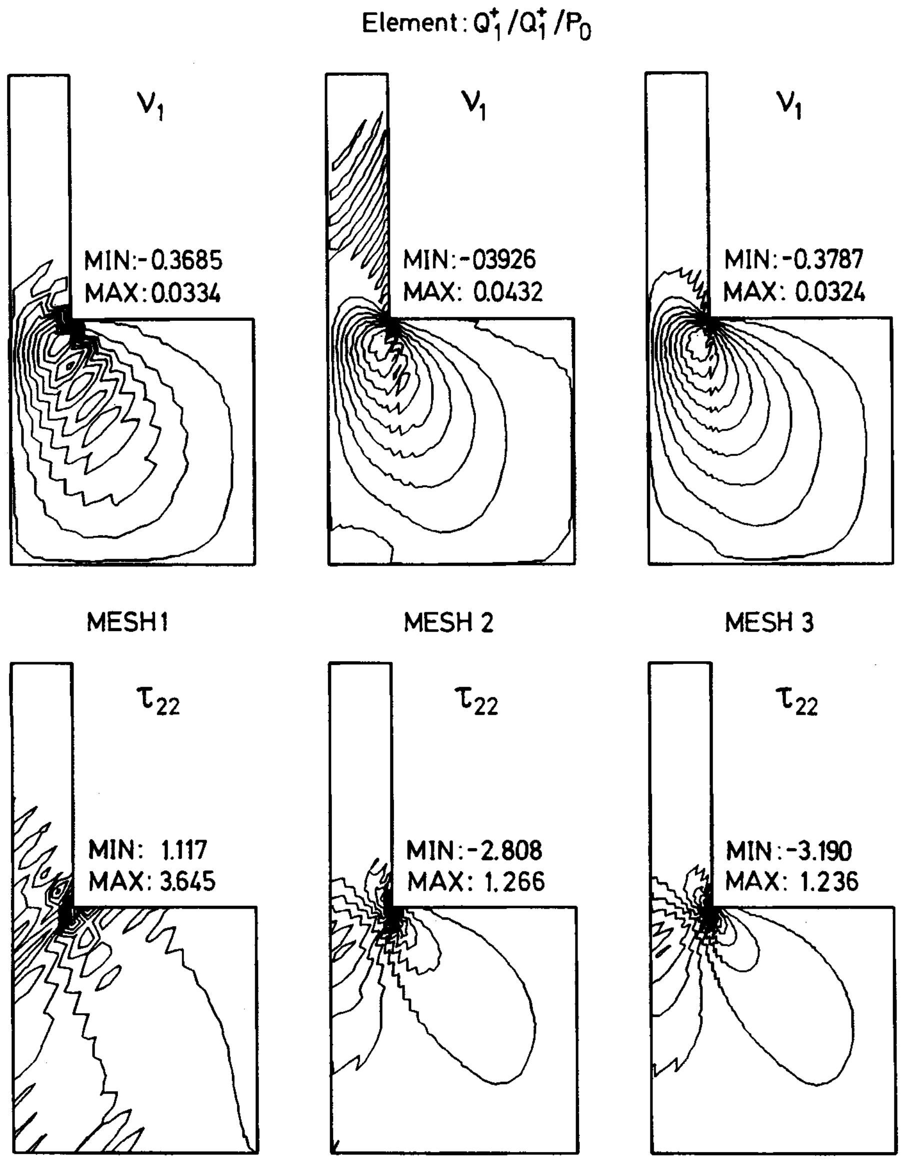

Figure 8. Performance of the $Q_1^+/Q_1^+/P_0$ element (as in Figure 3).

Let Ω be the square $[-1, 1] \times [-1, 1]$, and let us define on it the volumetric force

$$f = (-48x^2y^3 - 24x^4y + 36y, \quad 48x^3y^2 + 24xy^4 - 12x).$$

It is easily verified that the stream function and pressure

$$\psi = (1 - x^4)(1 - y^4), \qquad p = 12xy + C,$$

where C is an arbitrary constant, satisfy the dynamic equilibrium equations. The corresponding

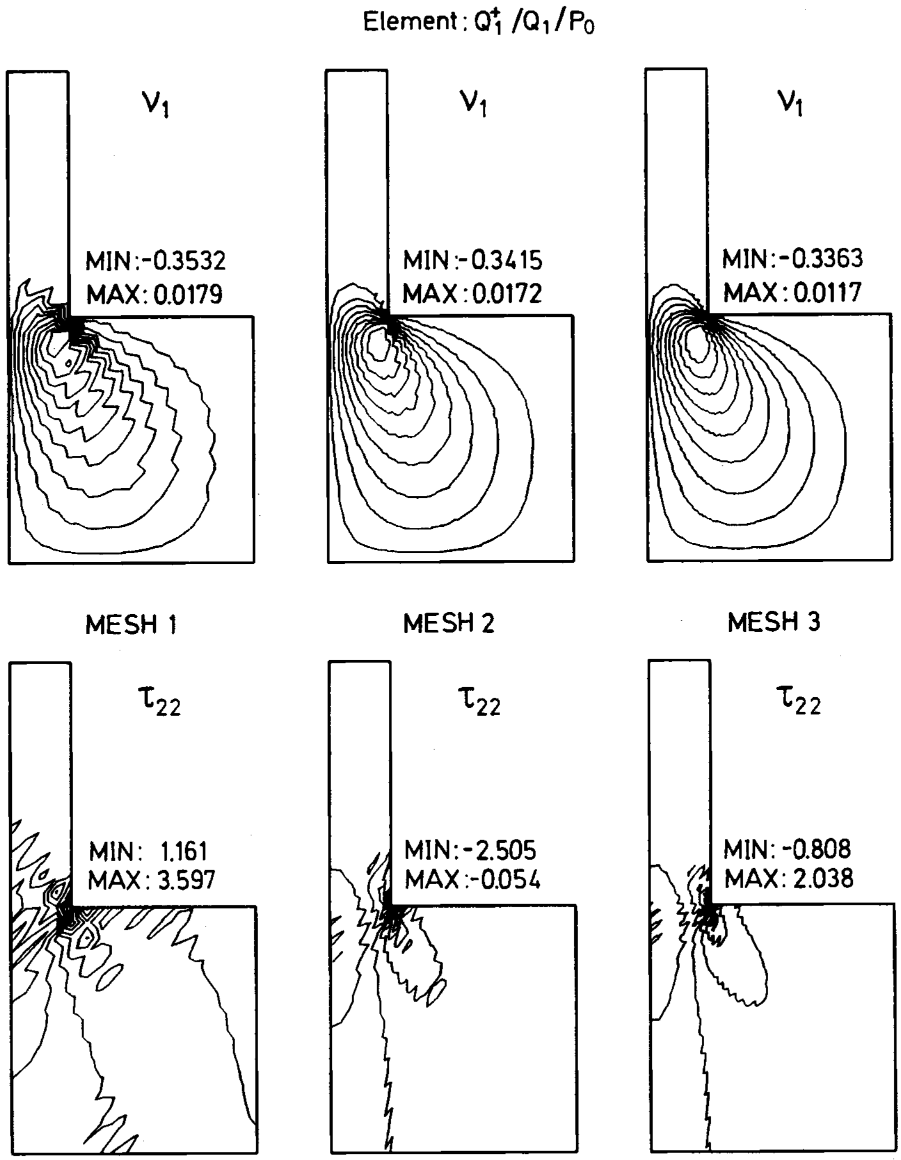

Figure 9. Performance of the $Q_1^+/Q_1/P_0$ element (as in Figure 3).

velocity and extra-stress fields are

$$v=[-4y^3(1-x^4),\ 4x^3(1-y^4)],$$

$$\tau_{11}=-\tau_{22}=32\mu_1 x^3 y^3,$$

$$\tau_{12}=12\mu_1[x^2(1-y^4)-y^2(1-x^4)].$$

We, thus, impose the boundary conditions on velocity that come from the above formula, and compute the $L^2(\Omega)$-norm of the true error by substracting the numerical solution from the exact one at each quadrature point. We have taken $\mu_1=0{\cdot}999$, $\mu_2=0{\cdot}001$, and exploited the symmetry to restrict the domain to $[0, 1]\times[0, 1]$.

The analysis was performed on three uniform meshes for each element, consisting of 121, 441 and 961 stress–velocity nodes (excluding bubbles) and the correspondng mesh sizes are proportional to 1/5, 1/10 and 1/15. These numbers are defined as h in our error plots. In Figures 10(a), 10(b) and 10(c), we show respectively, the error in extra-stress, velocity and pressure as functions of $1/h$. These results are in agreement with those of the previous sections. The elements under study can be classified into two groups: The *stable* ones ($Q_2/Q_2/P_1$, $P_2^+/P_2^+/P_1$, $Q_1/Q_1/P_0$ and $Q_1^+/Q_1/P_0$) which converge towards the exact solution with the expected order, and the *unstable* ones, which exhibit convergence orders well below the others.

We finish this section with a few remarks:

1. The numerical tests confirm that all elements recover the theoretical[1] convergence orders when $\mu_2>0{\cdot}2$.
2. The Q_1/P_0 combination for velocity and pressure, as is well-known (see e.g. Reference 10), does not satisfy the Babuska–Brezzi condition and, thus, is not a stable element. It is also known to yield pretty accurate results,[10] as in this case, which up to now resist analysis.
3. In view of the obtained results, the addition of a stress bubble to the $Q_1/Q_1/P_0$ does not seem worthy.
4. It is interesting to note that, although the $Q_2/Q_2/P_1$ and $P_2^+/P_2^+/P_1$ exhibit similar convergence behaviour in the regular problem considered, the former yields much more accurate results for a given mesh size.

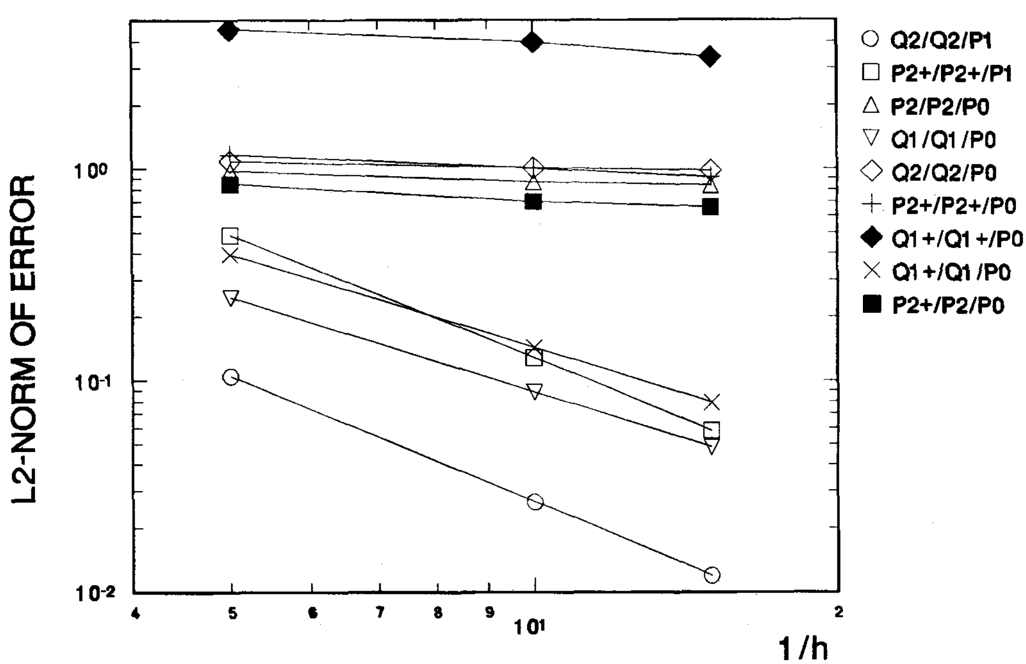

(a)

Figure 10. Numerical convergence analysis on the regular problem of Section 6. $L^2(\Omega)$-norms of errors in (a) extra-stress, (b) velocity and (c) pressure for nine mixed elements. The corresponding convergence orders (slopes) can be found in Table I

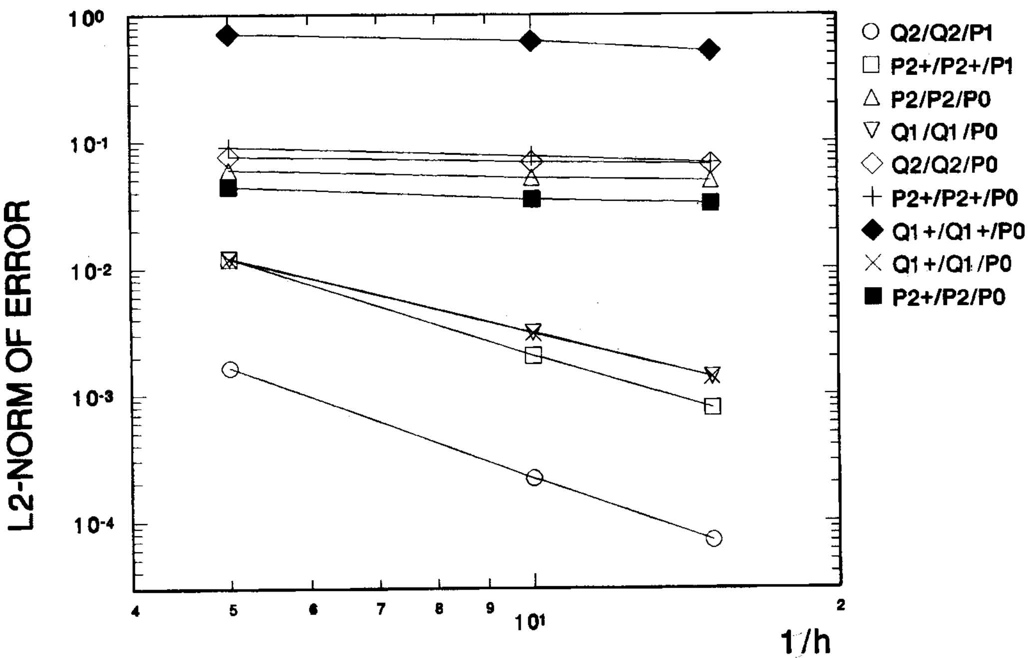

(b)

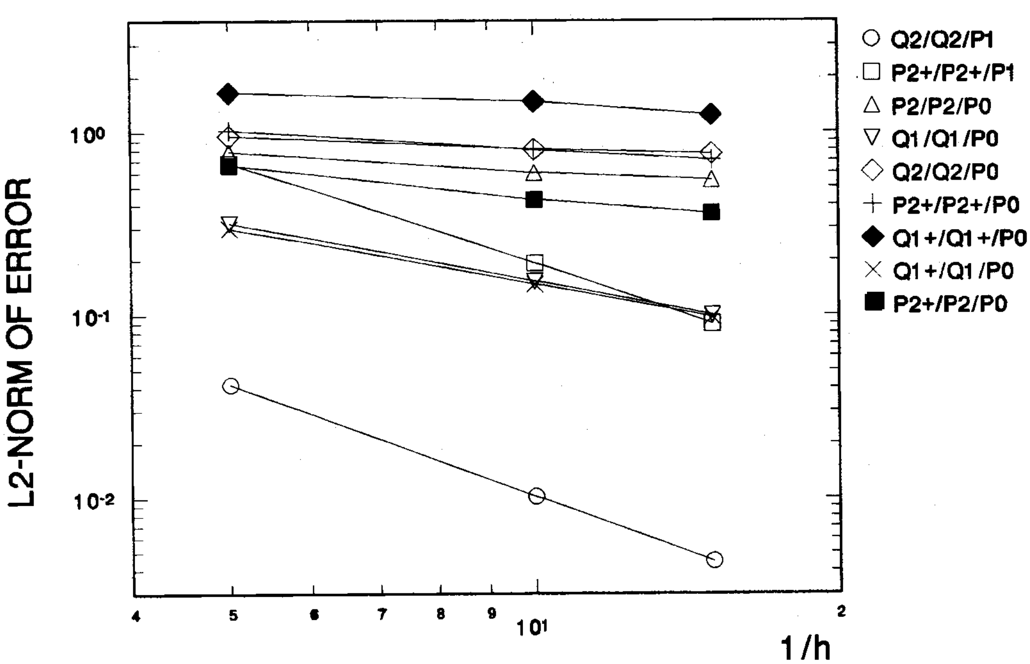

Figure 10. (Continued)

Table I.

Extra-stress element (continuous)	Velocity element (continuous)	Pressure element (discontinuous)	Convergence orders for the regular problem of Section 6 (L^2-norm)			Stable in the 4-to-1 contraction?
			τ	v	p	
Q_2	Q_2	P_1	~2·0	~2·8	~2·0	Yes?
Q_2	Q_2	P_0	~0·1	~0·1	~0·1	No
P_2^+	P_2^+	P_1	~2·0	~2·4	~1·9	Yes
P_2^+	P_2^+	P_0	~0·2	~0·3	~0·3	No
P_2^+	P_2	P_0	~0·1	~0·2	~0·4	No
P_2	P_2	P_0	~0·1	~0·1	~0·2	No
Q_1^+	Q_1^+	P_0	~0·4	~0·4	~0·4	No?
Q_1^+	Q_1	P_0	~1·5	~2·0	~1·0	No
Q_1	Q_1	P_0	~1·5	~2·0	~1·0	Yes?

7. DISCUSSION AND CONCLUDING REMARKS

It has been shown that, when μ_2 is small, the pressure discretization plays a crucial role in the stability of the discrete version of (4)–(6). A proper explanation for this can be found if the following two facts are recalled: first, that the μ_2 term in (4) can be thought of as a regularization term and, thus, problem (4)–(6) will yield erroneous results with μ_2 small if the problem is ill-posed when μ_2 vanishes (in analogy to what happens in nearly incompressible elasticity and in the penalized version of the velocity–pressure formulation of the Stokes problem with exact integration). Second, that the discrete pressure space enters the stability condition (7) via the definition of the space X_h. In fact, the smaller the Q_h the bigger is the X_h. As the *infimum* in (7) is taken over a larger space when Q_h is reduced, the stability constant can indeed be lower and perhaps zero. This explains the results of Section 5.1.

The small influence of the addition of usual bubble functions is also noteworthy, as it would have been attractive that such a simple modification of standard elements had a stabilizing effect on three-fields formulations. In References 2 and 8 some other special bubble functions are considered, which can serve for stability purposes.

Let us now summarize the behaviour of the elements under study with Table I. There, we collect the observations of Sections 4 and 5, together with the obtained convergence orders in the regular problem of Section 6. It is remarkable that the good convergence properties of the $Q_2/Q_2/P_1$ element are not verified in the 4-to-1 contraction problem. This could be an effect of the stress singularity, and is in agreement with the oscillations found with this element in the (also singular) stick–slip problem.[8]

Finally, the $P_2^+/P_2^+/P_1$ has exhibited a promising performance which should be confirmed by further tests. We are now carrying out similar comparisons with viscoelastic fluids, which are the content of a forthcoming paper.[11]

ACKNOWLEDGEMENTS

Pre- and post-processing was effected with the in-house codes ENREDO and PITUCO, kindly provided by M. J. Vénere, E. A. Dari and D. L. Arnica. Fruitful discussions with J. Baranger, F. G. Basombrío, R. Codina and C. Padra are gratefully acknowledged. The problem of Section 6 is a slight modification of the one suggested by V. Ruas to the author.

This work was partially supported by CONICET under PID-BID No. 39.

REFERENCES

1. J. Baranger and D. Sandri, 'Formulation of Stokes' problem and the linear elasticity equations suggested by Oldroyd model for viscoelastic flows', *Math. Modelling Numer. Anal.*, **26**, 331–345 (1992).
2. J. H. Carneiro de Araújo, *Tese de doutorado*, Pontificia Universidade Católica do Rio de Janeiro, 1991.
3. M. Fortin and R. Pierre, 'On the convergence of the mixed method of Crochet and Marchal for viscoelastic flows', *Comput. Methods Appl. Mech. Eng.*, **73**, 341–350 (1989).
4. L. Franca and R. Stenberg, 'Error analysis of some Galerkin–Least-squares methods for the elasticity equations', *Rapport de Recherche INRIA No. 1054*, 1989.
5. P. Le Tallec and M. Ravachol, 'Finite element approximation of viscoelastic progressively incompressible flows', *Numer. Math.*, **56**, 43–66 (1989).
6. J. M. Marchal and M. J. Crochet, 'Hermitian finite elements for calculating viscoelastic flow', *J. Non-Newtonian Fluid Mech.*, **20**, 187–207 (1986)
7. J. M. Marchal and M. J. Crochet, 'A new mixed finite element for calculating viscoelastic flow', *J. Non-Newtonian Fluid Mech.*, **26**, 77–114 (1987).
8. V. Ruas, J. H. Carneroi de Araújo and M. A. M. Silva Ramos, 'Computer simulation of viscoelastic flow using a new class of finite elements', in Ch. Hirsch *et al.* (eds), *Computational Fluid Dynamics Vol. 2*, Elsevier, Amsterdam, 1992, pp. 1039–1046.
9. M. A. Hulsen, 'A numerical method for solving steady 2D and axisymmetrical viscoelastic flow problems with an application to inertia effects in contraction flows', Delft Univ. Technol., Lab. Aero and Hydrodynamics, MEMT 11, 1990.
10. F. Brezzi and M. Fortin, *Mixed and Hybrid Finite Element Methods*, Springer, New York, 1991.
11. G. C. Buscaglia, 'A new coupled method for viscoelastic flow simulation' (1992), submitted.